Nevada Bureau of Mines and Geology Special Publication 36

Geophysical Setting of the February 21, 2008 M_w 6.0 Wells Earthquake, Nevada, Implications for Earthquake Hazards

by

Ponce, D.A., Watt, J.T., and Bouligand, C.
U.S. Geological Survey, Menlo Park, CA

2011

ABSTRACT

We utilize gravity and magnetic methods to investigate the regional geophysical setting of the Wells earthquake. In particular, we delineate major crustal structures that may have played a role in the location of the earthquake and discuss the geometry of a nearby sedimentary basin that may have contributed to observed ground shaking. The February 21, 2008 M_w 6.0 Wells earthquake, centered about 10 km northeast of Wells, Nevada, caused considerable damage to local buildings, especially in the historic old town area. The earthquake occurred on a previously unmapped normal fault and preliminary relocated events indicate a fault plane dipping about 55 degrees to the southeast. The epicenter lies near the intersection of major Basin and Range normal faults along the Ruby Mountains and Snake Mountains, and strike-slip faults in the southern Snake Mountains.

Regionally, the Wells earthquake epicenter is aligned with a crustal-scale boundary along the edge of a basement gravity high that correlates to the Ruby Mountains fault zone. The Wells earthquake also occurred near a geophysically defined strike-slip fault that offsets buried plutonic rocks by about 30 km. In addition, a new depth-to-basement map, derived from the inversion of gravity data, indicates that the Wells earthquake and most of its associated aftershock sequence lie below a small oval- to rhomboid-shaped basin, that reaches a depth of about 2 km. Although the basin is of limited areal extent, it could have contributed to increased ground shaking in the vicinity of the city of Wells, Nevada, due to basin amplification of seismic waves.

INTRODUCTION

The February 21, 2008 M_w 6.0 earthquake occurred about 10 km northeast of Wells, a small city (population about 1350) in northern Nevada along Interstate 80 (figure 1), situated at the base of the Ruby Mountains-East Humboldt Range. Residents reported about 20–40 seconds of shaking (dePolo, 2008) that resulted in considerable damage to local buildings, especially unreinforced masonry structures in the historic downtown area (figure 2).

The Wells earthquake was located at lat 41.1601N. long. -114.8771W. lat. (NAD27) at a depth of 8.0 km (Nevada Seismological Laboratory, 2008) in a region of low historical seismicity (inset, figure 1) and low seismic hazard (Petersen and others, 2008). The earthquake occurred on a previously unknown north-northeast-trending normal fault dipping about 55 degrees to the southeast that did not rupture the surface (e.g., dePolo, 2008; Smith and others, this volume) and may correspond to a previously unrecognized segment of the Clover Hill fault, a north-south striking normal fault on the east side of the Ruby Mountains-East Humboldt Range (Henry and Colgan, this volume). The epicenter also lies near the intersection of major Basin and Range normal faults along the Ruby Mountains and Snake Mountains (Stewart and Carlson, 1978), the Cedar Peak fault zone in the southern Snake Mountains (Thorman, 2003; Thorman and Brooks, this volume), and possibly the Wells fault, a presumed strike-slip fault located between the East Humboldt Range and the Snake Mountains (Thorman, 1970).

Here, we use gravity and magnetic methods to investigate the regional geophysical setting of the Wells earthquake as an aid in assessing the seismic hazard in northeast Nevada. Boundary analysis of gravity and magnetic data was used to help locate the edges of crustal structures that may have influenced the location of the Wells earthquake. In addition, an

iterative gravity inversion technique was used to determine the depth to basement rocks in order to delineate the geometry of nearby sedimentary basins and changes in basement geology.

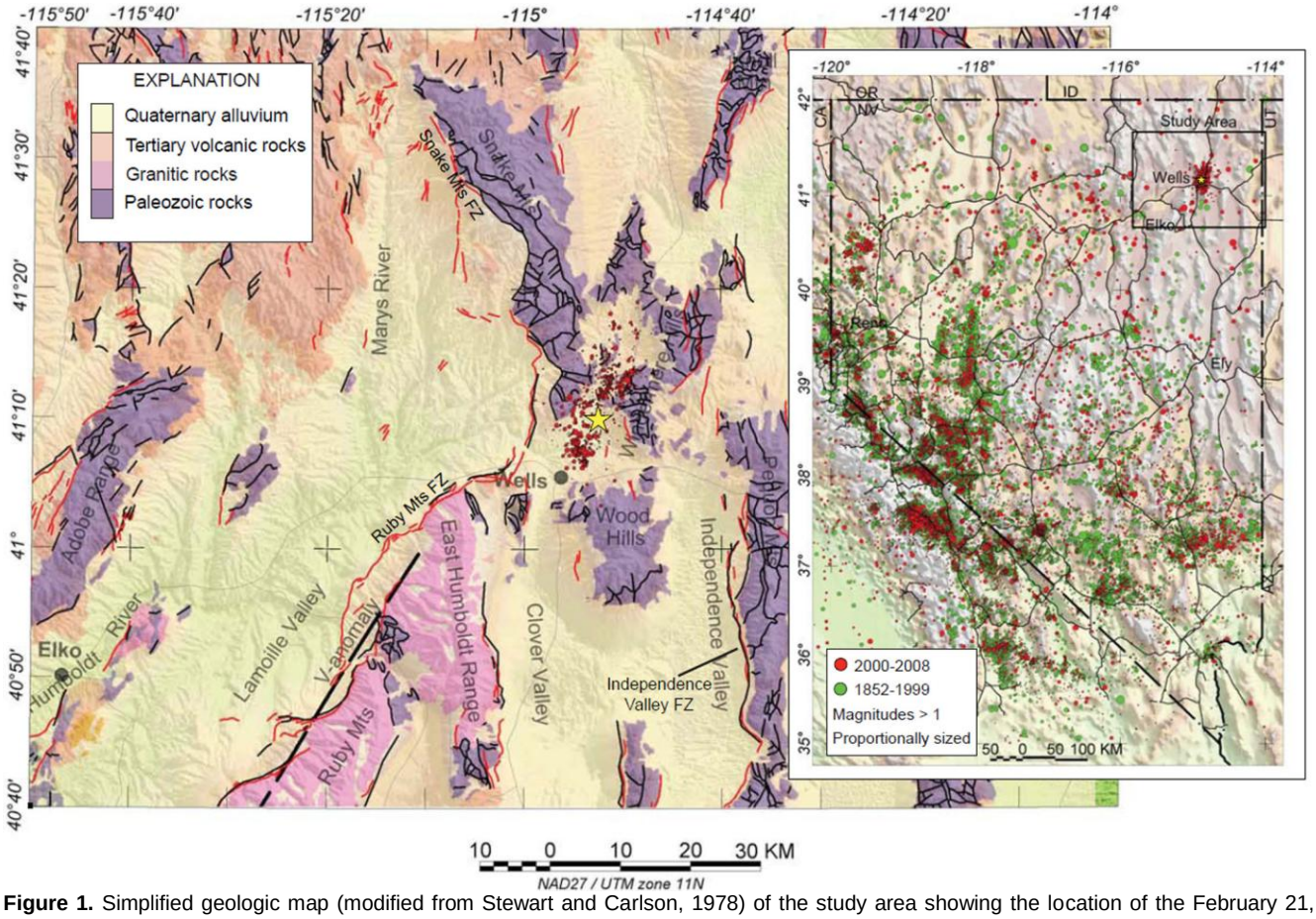

Figure 1. Simplified geologic map (modified from Stewart and Carlson, 1978) of the study area showing the location of the February 21, 2008 Wells M_w 6.0 earthquake and its aftershocks. Yellow star, Wells earthquake; red circles, relocated double-difference seismicity (K. Smith, University of Nevada Seismological Laboratory, written commun., 2008); red lines, Quaternary faults from Dohrenwend and others (1996); black lines, faults from Stewart and Carlson (1978); dashed black line, V-anomaly; gray lines, major roads. Inset: Earthquakes in Nevada (e.g., dePolo and dePolo, 1999; University of Nevada at Reno Seismological Laboratory earthquake catalog, 2008).

GEOPHYSICAL DATA AND METHODS

Gravity and Magnetic Data

An isostatic gravity map of the study area (figure 3) was derived from a statewide gravity data compilation of Nevada (Ponce, 1997) that was augmented with new gravity stations collected by the U.S. Geological Survey throughout northern Nevada, including about 90 gravity stations that we collected in the vicinity of the Wells earthquake during the spring and summer of 2008 (inset, figure 3). All gravity data were reduced using standard gravity methods (e.g., Dobrin and Savit, 1988; Blakely, 1995) and include an isostatic gravity correction. The resulting isostatic anomaly is particularly useful because it emphasizes features in the mid- to upper crust by removing long-wavelength variations in the gravity field related to the isostatic compensation of topography (e.g., Jachens and Roberts, 1981; Simpson and others, 1986). Gravity values are reported in milligals (mGal), equivalent to an acceleration of 10^{-5} m/s^2.

Figure 2. Photographs showing the extensive damage to the historic old town area on Front Street, Wells, Nev. (photos by D.A. Ponce).

An aeromagnetic map of the study area (figure 4) was derived from a statewide updated compilation of Nevada by Kucks and others (2006). Aeromagnetic data were corrected by Kucks and others (2006) for diurnal variations of the Earth's magnetic field, upward or downward continued to a constant elevation of 305 m above the ground, adjusted to a common datum, and merged to produce a uniform map with a grid spacing of 500 m. This improved compilation, although composed of surveys acquired with different specifications, allows interpretation of magnetic anomalies across survey boundaries (Kucks and others, 2006).

Aeromagnetic surveys over the Wells study area have poor to fair spatial resolutions with a flight-line spacing of 5 km and a flight-line altitude of 150 m above the ground in the eastern two-thirds of the study area, and a flight-line spacing of 1.6 km and a flight-line altitude of 2.7 km at a constant barometric altitude in the western third of the study area. Because of widely spaced surveys in the eastern part of the study area and high flight-line altitudes in the western part of the study area, some shallow magnetic sources may not be displayed in the aeromagnetic map. However, these issues are not significant for the regional-scale magnetic interpretations presented here.

Boundary Analysis

A directional derivative technique was used to locate maximum horizontal gradients of gravity data (R.W. Simpson, oral commun., 2006), which are likely to occur over abrupt lateral changes in the density of the underlying rock units, especially for shallow sources with steep edges (e.g., Cordell and Grauch, 1985; Blakely and Simpson, 1986; Blakely, 1995). Because the regional magnetic field and the direction of magnetizations are seldom vertical, magnetic anomalies are commonly laterally displaced from their sources and often have a more complex shape than gravity anomalies. For these reasons, magnetic data were first transformed into their magnetic potential (or pseudogravity) (e.g., Blakely, 1995) prior to horizontal gradient analysis. As a consequence, locations of maximum horizontal gradients of magnetic data shown in figure 4 are shifted with respect to the apparent edges of the non-transformed magnetic anomalies. Alignments of maximum horizontal gradient locations obtained from both gravity and magnetic data (open circles, figs. 3 and 4) were used as a proxy for lineaments, faults, and boundaries of geologic features or geophysical terranes.

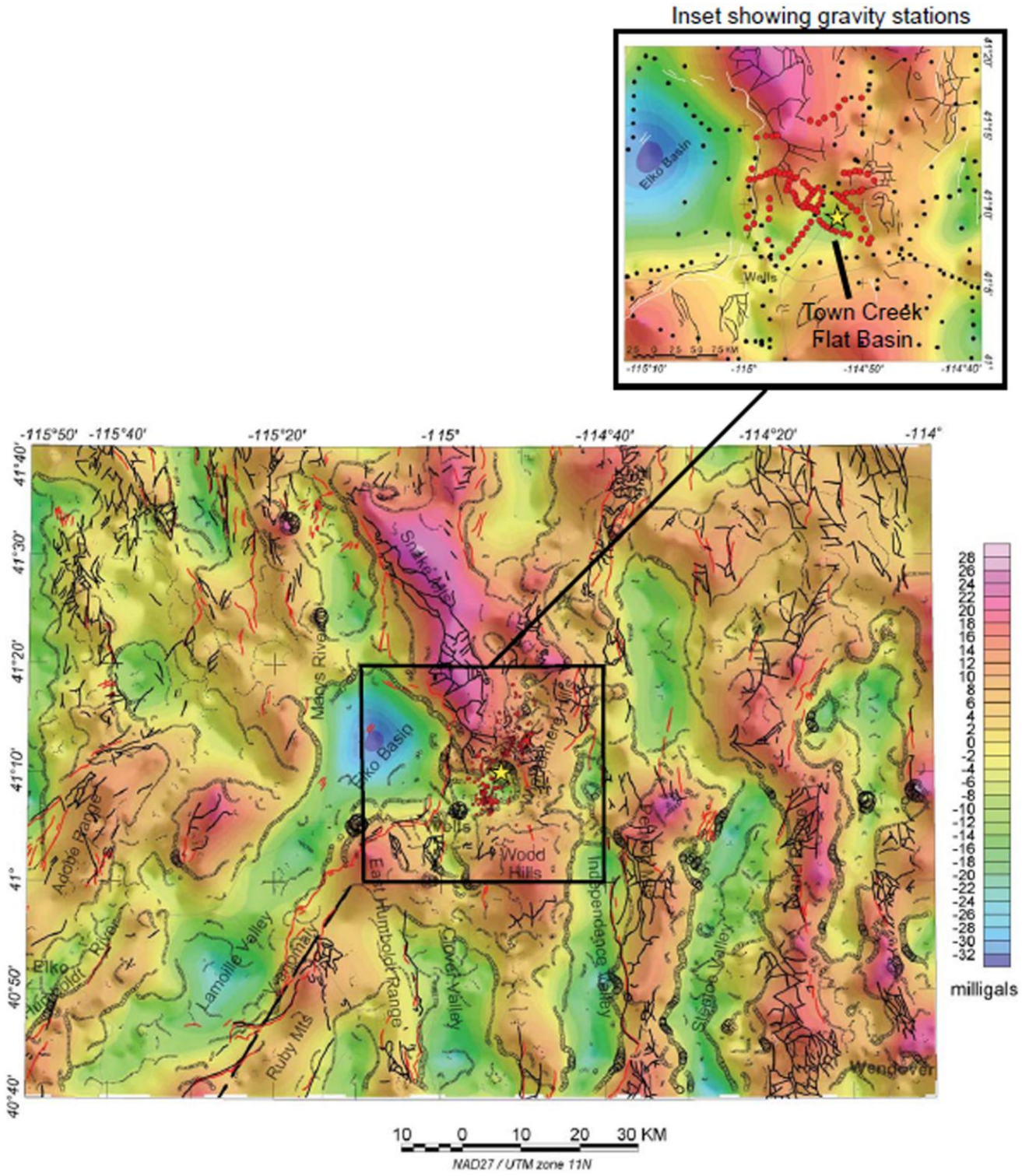

Figure 3. Isostatic gravity map of the study area. Black circles proportionally-sized maximum horizontal gradient locations. See figure 1 for additional explanation. Inset: isostatic gravity map showing gravity station locations. Red circle, new gravity station; black circle, pre-existing gravity station.

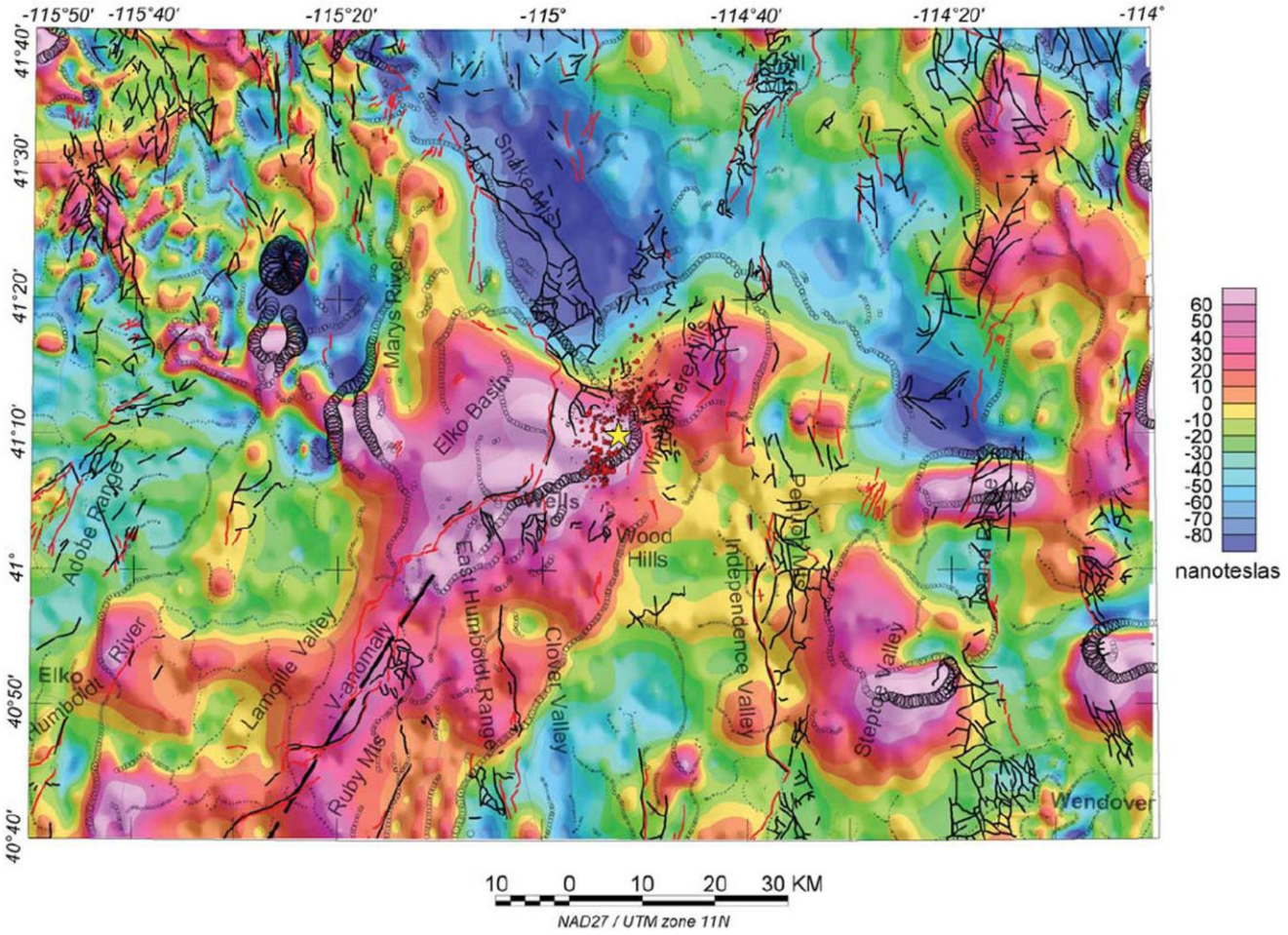

Figure 4. Aeromagnetic map of the study area (from Kucks and others, 2006). Black circles proportionally-sized maximum horizontal gradient locations. See figure 1 for additional explanation.

Gravity Inversion

The isostatic gravity map (figure 3) includes anomalies due to both basement rocks and basin-fill deposits, the effect of the latter often obscuring the former. In order to emphasize gravity anomalies associated with pre-Cenozoic basement rocks, we used an improved iterative gravity inversion method (B. Chuchel, written commun., 2008) originally developed by Jachens and Moring (1990). The inversion process separates the isostatic gravity field into two components: the gravity field generated by pre-Cenozoic basement (and intrusive) rocks and the gravity field generated by less-dense Cenozoic deposits. The resulting basement gravity field can be used to identify geophysical features within the basement rocks (figure 5) and the resulting basin gravity field can be used to determine the thickness of Cenozoic deposits (or depth to basement) in the study area (figure 6a). The gravity inversion was constrained by simplified surficial geologic data (modified from Stewart and Carlson, 1978), a density-depth function for lower-density Cenozoic deposits derived by Jachens and Moring (1990) from borehole and physical property data; and a number of drill holes (black circles, figure 6a) that reach basement (e.g., Hess, 2004). Note that none of these drill holes are located in the small basin just northeast of Wells, herein referred to as the Town Creek Flat basin (figs. 6a, b). The resulting depth to basement and basement gravity maps account well for the gravity map as residual anomalies not taken into account by our separation process are very small (about 0.2 mGal) compared to the amplitude of gravity anomalies in the area (about 30 mGal).

Because of the nonuniqueness of potential-field methods (e.g., Blakely, 1995), other more complex basement and basin models could also account for the observed gravity field. Uncertainties in the depth to basement process can also arise from inaccuracies in the density-depth function, sparse gravity data control (especially on basement outcrops), and limited independent constraint information (e.g., Jachens and Moring, 1990; Saltus and Jachens, 1995). Because of these limitations, caution should be exercised when interpreting basin thicknesses more accurate than about 200 to 500 m.

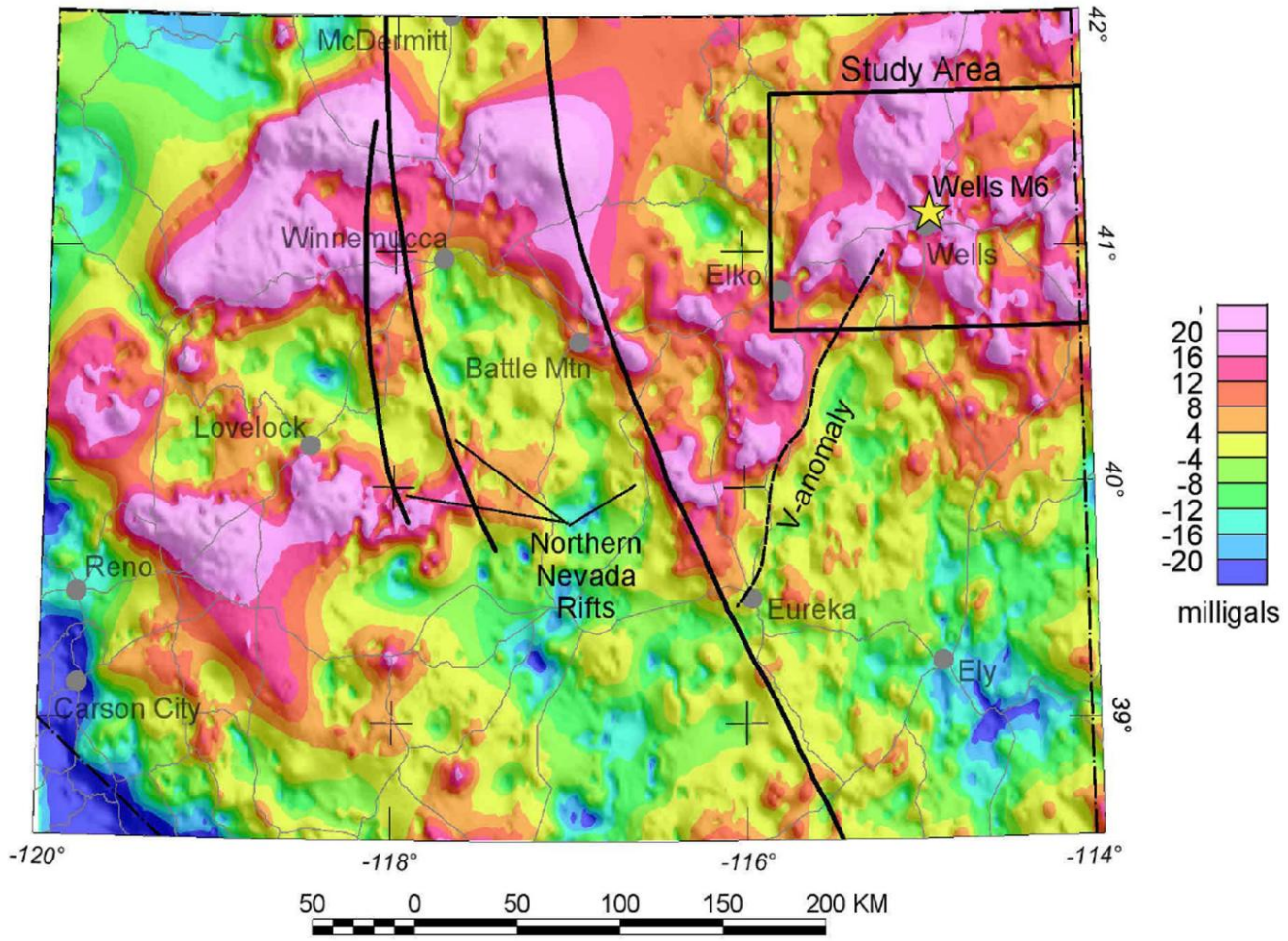

Figure 5. Regional gravity map of northern Nevada showing gravity anomalies associated with pre-Cenozoic basement rock, derived from the inversion of gravity data. Black bold dashed-line, crustal boundary on east side of a V-shaped basement gravity high (e.g., Ponce and Glen, 2008); black lines, northern Nevada rifts; gray lines, major roads. See figure 1 for additional explanation.

GEOPHYSICAL SETTING

The isostatic gravity map of the study area (figure 3) is dominated by a series of gravity highs and lows that in general, reflect dense Paleozoic rock outcrops and low-density basin deposits, respectively. High gravity values occur over the Snake Mountains, which are composed of a thick section of Paleozoic and possibly Precambrian rocks, whereas a relatively lower-amplitude gravity high over the Ruby Mountains may reflect lower-density plutonic rocks that compose much of the mountain (Howard, 2003). However, this subdued gravity high may also be partly related to the poor gravity station coverage over the rugged and remote Ruby Mountains. The lowest isostatic gravity values are associated with the Elko basin, a relatively deep sedimentary basin along the western margin of the Ruby Mountains-East Humboldt Range (e.g., Wallace and others, 2008). Of particular interest to this study is a gravity low associated with the Town Creek Flat basin, a small basin northeast of Wells between the Snake Mountains and the Windermere Hills.

The magnetic map of the study area (figure 4) is dominated by a broad long-wavelength high-amplitude anomaly probably associated with plutonic rocks along the Ruby Mountains-East Humboldt Range. High-amplitude short-wavelength anomalies are associated with volcanic rocks in the northwest corner of the map. Magnetic anomalies are particularly useful for delineating the subsurface extent of plutonic rocks (e.g., Grauch and others, 1988), because plutons are often fairly magnetic compared to the basement rocks they intrude. The extent of plutonic rocks in the study area was delineated by comparing the location of maximum horizontal gradients around broad long-wavelength magnetic anomalies with the location of plutonic rock outcrops. Combined, these data reveal that north-northeast-trending plutonic rocks associated with the Ruby Mountains-East Humboldt Range extend uninterrupted beneath the city of Wells and abruptly terminate along a prominent north-northwest trending magnetic lineament (figure 4). A nose of this magnetic anomaly extends northeastward over the Windermere Hills, suggesting that plutonic rocks are present at depth here as well.

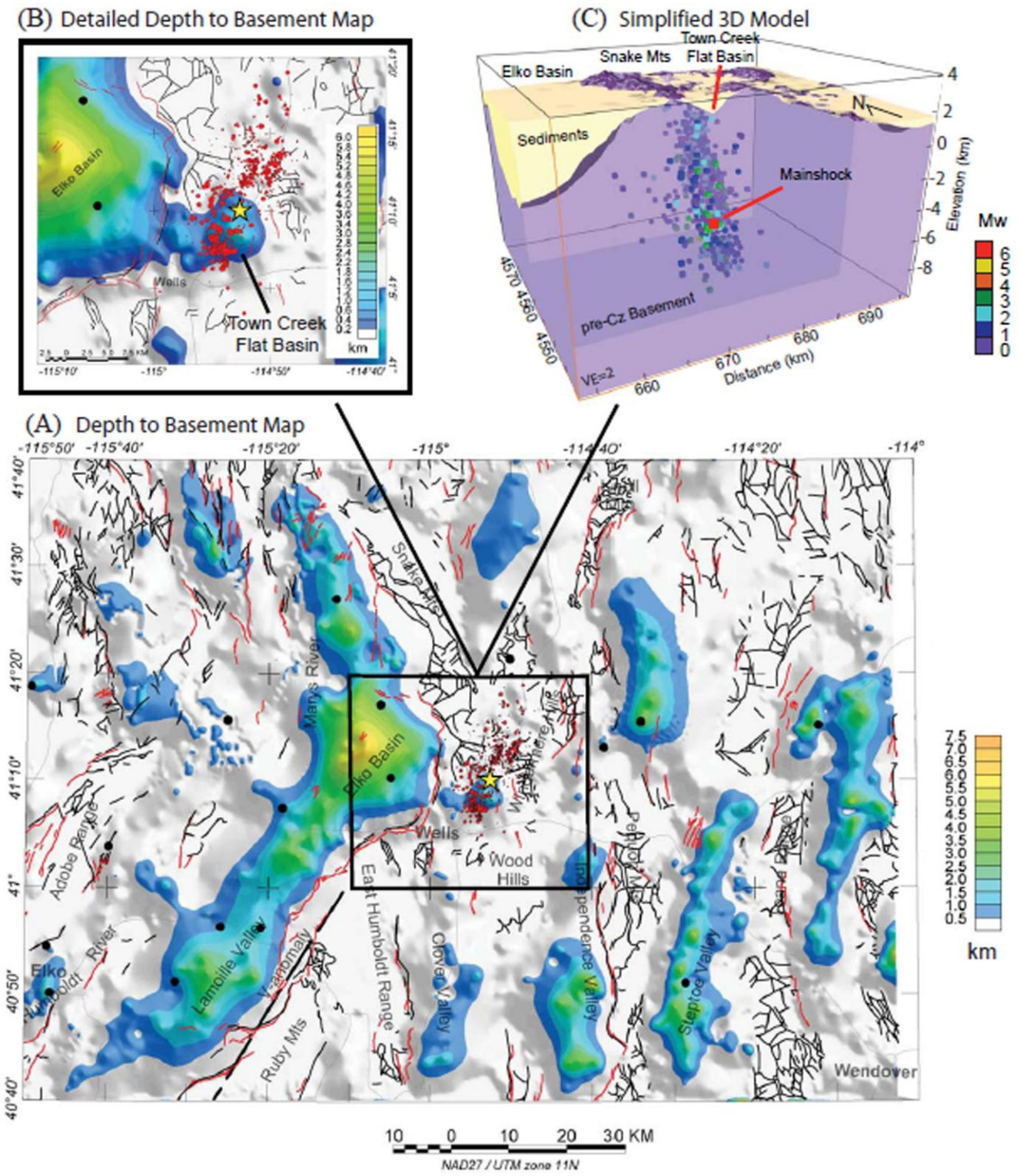

Figure 6. (A) Depth to basement map showing the depth to pre-Cenozoic rocks (or the thickness of basin-fill deposits) derived from the inversion of gravity data, (B) Detailed depth to basement map, and (C) 3D model of the epicentral region. See figure 1 for additional explanation. Black circles, drill holes that penetrate pre-Cenozoic basement.

In the vicinity of Wells, the magnetic anomaly associated with the Ruby Mountains-East Humboldt Range is fairly broad and extends below the deepest parts of the Elko basin, which indicates that its causative source is relatively deep (>5 km). In addition, exposed plutonic rocks along the Ruby Mountains-East Humboldt Range are peraluminous granitic rocks and only weakly magnetic, which further suggests that the source of the broad magnetic anomaly is probably a deeper and more mafic pluton or alternatively, some other type of magnetic crystalline basement.

The basement gravity map of northern Nevada (figure 5) is dominated by a gravity high sweeping across the northern part of the state, whose edges probably reflect crustal-scale geophysical boundaries or features. In particular, the epicenter of the Wells earthquake is approximately on strike with a crustal boundary on the east side of a V-shaped part of this basement gravity high (Ponce and Glen, 2008). The northeastern limb of the 'V' coincides with the western margin of the Ruby Mountains-East Humboldt Range and marks a major crustal-scale change in basement lithology along the Ruby Mountains fault zone with higher gravity values (i.e., densities) to the north. The western margin of the V-shaped basement gravity high (figure 5) correlates to one of the most prominent geophysical features in Nevada, the northern Nevada rift (e.g., Zoback and others, 2004 and references therein), a mafic intrusion related to the inception of the approximately 16 Ma Yellowstone Hotspot, that may have in part, followed this pre-existing basement feature (Ponce and Glen, 2008).

The depth–to-basement map of the Wells area (figure 6a) is dominated by the Elko basin that consists of a series of NNE-trending sub-basins (described in detail by Wallace and others, 2008). These sub-basins are along the western margin of the Ruby Mountains from Elko to northwest of Wells. The Wells earthquake lies just east of the deepest sub-basin within a small (8 x 10 km) oval- to rhomboid-shaped basin situated between the Snake Mountains and Windermere Hills. This basin is separated from the Elko Basin by a buried ridge of basement rocks. A more detailed depth-to-basement map (figure 6b) indicates that the Town Creek Flat basin is asymmetric and reaches a depth of about 1.8 km along its eastern margin.

DISCUSSION

Combined gravity and magnetic data (figs. 4 and 5) indicate that the Wells earthquake occurred near the intersection of two major geophysical features (figure 7), the northeast-trending basement gravity anomaly along the Ruby Mountains fault zone and a magnetic anomaly that abruptly terminates along a sharply defined magnetic lineament or fault. Although the earthquake did not occur on these faults, the intersection of these structures may have played a role in the regional stress regime influencing the Wells M_w 6.0 earthquake.

The broad basement gravity high in northeastern Nevada (figure 5) probably reflects a transition from predominantly Paleozoic crust in the southwest to Precambrian crust in the northeast, but could also be related to mid- to sub-crustal mafic intrusions (Ponce and Glen, 2008). Some of these basement gravity highs may indicate the presence of dense Archean cratonic crust whose existence in northeast Nevada was suggested by several studies (e.g., Tosdal and others, 2000; Reed, 1993; Sims and others, 2005, and references therein). In particular, the Archean-Proterozoic suture zone has been inferred just north of the Wells area based on magnetotelluric soundings (Rodriguez and Williams, 2008). Also, Lush and others (1988) described ortho- and paragneisses exposed along the eastern flank of the East Humboldt Range as Archean. However, recent age-dating by Premo and others (2008) preclude an Archean age for these rocks, showing that they are Late Cretaceous monzogranite derived from sedimentary rocks with a predominantly Archean detrital source.

The magnetic lineament that terminates the broad magnetic anomaly associated with the Ruby Mountains-East Humboldt Range north of Wells is observed over a distance of at least 50 km and appears to offset a prominent nose of the magnetic anomaly that extends over the Windermere Hills (figs. 4 and 7). This offset indicates that the lineament probably reflects a right-lateral strike-slip fault with a displacement of about 20-30 km that has truncated the deep source of the magnetic anomaly, an inferred pluton beneath the Ruby Mountains-East Humboldt Range. The steep and linear northern margin of the Elko basin, based on gravity data, also abruptly terminates along this magnetic lineament. In addition, recent magnetotelluric studies in northeast Nevada (Rodriguez and Williams, 2008) imaged a broad conductive zone extending 20-km deep, that they related to the Wells fault, and which terminates near our geophysically defined fault. Combined, these data indicate the existence of a linear and nearly vertical fault that extends over a distance of at least 50 km, extends to great depths, and has up to about 30 km of right-lateral strike-slip offset.

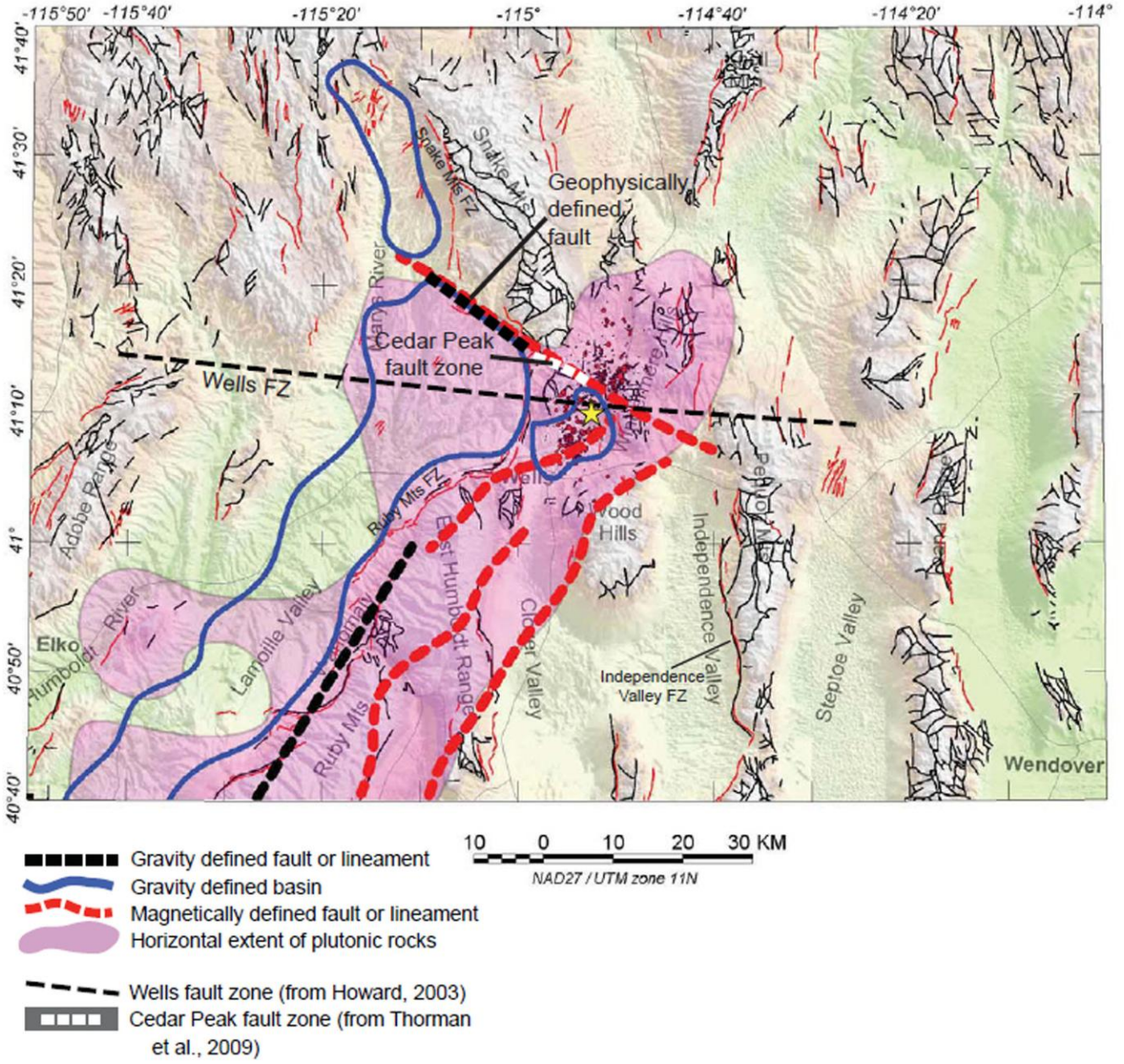

Figure 7. Geophysically defined lineaments and structures possibly associated with the February 21, 2008 Wells M_w 6.0 earthquake. See figure 1 for additional explanation.

This geophysically defined fault cuts across basement rock outcrops in the southern part of the Snake Mountains for a distance of only about 6-8 km, elsewhere it lies beneath alluvium, which may explain why this prominent feature was not recognized earlier. Several strike-slip faults have been identified in the southern part of the Snake Mountains (Thorman and others, 2003; Thorman and Brooks, this volume). In particular, the Cedar Peak fault system which is directly on strike with the magnetic lineament could possibly correspond to the exposed portion of the geophysically defined fault (figure 7). If so, it would mean that the Cedar Peak fault is a major geologic structure that extends to great depth and can be tracked for over 50 km. Alternatively, the geophysically defined fault may be related to another fault system, the Wells fault, a presumed strike-slip fault between the East Humboldt Range and the Snake Mountains (e.g., Thorman 1970; Thorman and others, 1991; Howard, 2003). Although the Wells fault is not exposed, it was inferred from offset by as much as 70 km between allocthons and geologic facies observed in the Adobe Range and the Snake Mountains (Thorman, 1970; Thorman and Ketner, 1979). The Wells fault may represent a transfer or accommodation zone that bounds the highly extended Ruby Mountains-East Humboldt Range core complex to the south (Howard, 2003). In either case, the intersection of this prominent geophysically defined fault with the Wells earthquake fault probably influenced the location of the Wells earthquake, and may have served as its nucleation site.

The Wells earthquake and the southern half of its associated aftershock sequence occurred below the oval Town Creek Flat basin that formed in response to active extension in the region. This basin reaches a depth of about 2 km, which is typical of many basins throughout Nevada, but quite deep considering its small areal extent (8 x 10 km). A simplified 3D geologic model of the basin (figure 6c) indicates that the Wells earthquake occurred on a southeast-dipping fault located along its western boundary. The city of Wells itself lies at the very southern edge of the basin and experienced considerable ground shaking during the Wells earthquake. Although proximity to the epicenter and rupture directivity (Dreger and others, 2008) are important factors for the observed ground shaking at Wells, the Town Creek Flat basin may have also played an important role. Even though the basin is of limited areal extent, its depth and geometry could have contributed to increased ground shaking due to basin-edge amplification of surface waves or focusing of deeper seismic waves (e.g., Hartzell, 1997; Graves and others, 1998; McPhee and others, 2007; and references therein). For example, in Santa Rosa, Calif., increased damage and ground motions during both the 1906 San Francisco earthquake and the 1969 Santa Rosa earthquakes were coincident with the edge of the Santa Rosa basin, a 2-km deep basin defined by the inversion of gravity data (McPhee and others, 2007). Indeed, seismic studies of the Wells earthquake (Petersen and others, 2008) indicate increased ground motion compared to predictions from Next Generation Attenuation ground motion equations (e.g., Abrahamson and Silva, 2008). Additional ground motion studies could help constrain possible basin-edge and basin-depth effects. Nevertheless, an M_w 6.0 earthquake in this previously seismically quiescent part of northeast Nevada indicates that Basin and Range normal faults are active in the region and capable of generating large damaging earthquakes.

ACKNOWLEDGMENTS

We would like to thank the University of Nevada Seismological Laboratory for making Nevada earthquake catalog data publically available on-line and Ken Smith for providing relocated double-difference seismicity data of the Wells earthquake and its aftershocks. We would also like to thank Joe Colgan, Chris Henry, Keith Howard, Darcy McPhee, Dan Scheirer, and Chuck Thorman for valuable discussions or reviews that improved the manuscript.

REFERENCES

Abrahamson, N.A., and Silva, W.J., 2008, Summary of the Abrahamson & Silva NGA ground-motion relations: Earthquake Spectra, v. 24, no. 1, p. 67–97.

Blakely, R.J., 1995, Potential theory in gravity and magnetic applications: Cambridge University Press, 441 p.

Blakely, R.J., and Simpson, R.W., 1986, Approximating edges of source bodies from gravity or magnetic data: Geophysics, v. 51, p. 1494–1498.

Cordell, L., and Grauch, V.J.S., 1985, Mapping basement magnetization zones from aeromagnetic data in the San Juan Basin, New Mexico, *in* Hinze, W.J., ed., The utility of regional gravity and magnetic anomaly maps: Society of Exploration Geophysicists, Tulsa, Oklahoma, p. 181–197.

dePolo, C.M., 2008, The 21 February 2008 Wells, Nevada, USA Earthquake—impacts of a major background earthquake on a rural community [abs.]: EOS (Transactions of the American Geophysical Union), v. 89, no. 53, abstract #S51B-1739.

dePolo, D.M., and dePolo, C.M., 1999, Earthquakes in Nevada, 1852–1998: Nevada Bureau of Mines and Geology Map 119, scale 1:1,000,000.

Dobrin, M.B., and Savit, C.H., 1988, Introduction to Geophysical Prospecting (4th ed.): New York, McGraw-Hill, 867 p.

Dohrenwend, J.C., Schell, B.A., Menges, C.M., Moring, B.C., and McKittrick, M.A., 1996, Reconnaissance photogeologic map of young (Quaternary and late Tertiary) faults in Nevada, *in* Singer, D.A., ed., An analysis of Nevada's metal-bearing mineral resources: Nevada Bureau of Mines and Geology Open-File Report 96-2, p. 9-1–9-12.

Dreger, D.S., Ford, S.R., and Ryder, I., 2008, Finite-source study of the February 21, 2008 M_w 6.0 Wells, Nevada, Earthquake [abs.]: EOS (Transactions of the American Geophysical Union), v. 89, no. 53, abstract #S51B-1743.

Grauch, V.J.S., Blakely, R.J., Blank, H.R., Oliver, H.W., Plouff, Donald, and Ponce, D.A., 1988, Geophysical delineation of granitic plutons in Nevada: U.S. Geological Survey Open-File Report 88-11, 7 p., 2 plates, scale 1:1,000,000.

Graves, R.W., Arben, P., and Somerville, P.G., 1998, Ground motion amplification in the Santa Monica area—effects of shallow basin edge structure: Bulletin of the Seismological Society of America, v. 88, p.1224–1242.

Hartzell, S., Cranswick, E., Frankel, A., Carver, D., and Meremonte, M., 1997, Variability of site response in the Los Angeles urban area: Bulletin of the Seismological Society of America, v. 87, no. 6, p. 1377–1400.

Henry, C.D., and Colgan, J.P., 2009, *this volume*, The regional structural setting of the 2008 Wells earthquake and Town Creek Flat basin—implication for the Wells earthquake fault and adjacent structures.

Hess, R.H., 2004, Nevada oil and gas well database: Nevada Bureau of Mines and Geology Open-File Report 04-1, 288 p.

Howard, K.A., 2003, Crustal structure in the Elko-Carlin region, Nevada during Eocene gold mineralization—Ruby-East Humboldt metamorphic core complex as a guide to the deep crust: Economic Geology, v. 98, p. 249–268.

Jachens, R.C., and Moring, B.C., 1990, Maps of the thickness of Cenozoic deposits and the isostatic residual gravity over basement for Nevada: U.S. Geological Survey Open-File Report 90-404, 15 p.

Jachens, R.C., and Roberts, C.W., 1981, Documentation of a FORTRAN program, 'isocomp', for computing isostatic residual gravity: U.S. Geological Open-File Report 81-574, 26 p.

Kucks, R.P., Hill, P.L., and Ponce, D.A., 2006, Nevada magnetic and gravity maps and data—a website for the distribution of data: U.S. Geological Survey Data Series 234. [http://pubs.usgs.gov/ds/2006/234].

Lush, A.P., McGrew, A.J., Snoke, A.W., and Wright, J.E., 1988, Allochthonous Archean basement in the northern East Humboldt Range, Nevada: Geology, v. 16, p. 349–353.

McPhee, D.K., Langenheim, V.E., Hartzell, S., McLaughlin, R.J., Aagaard, B.C., Jachens, R.J., and McCabe, C., 2007, Basin Structure beneath the Santa Rosa Plain, northern California—implications for damage caused by the 1969 Santa Rosa and 1906 San Francisco earthquakes: Bulletin of the Seismological Society of America, v. 97, no. 5, p. 1449–145.

Nevada Seismological Laboratory, 2008, Earthquake catalog: University of Nevada at Reno, Nevada. [http://www.seismo.unr.edu/Catalog/catalog-search.html].

Petersen, M.D., Frankel, A.D., Harmsen, S.C., Mueller, C.S., Haller, K.M., Wheeler, R.L., Wesson, R.L., Zeng, Y., Boyd, O.S., Perkins, D.M., Luco, N., Field, E.H., Wills, C.J., and Rukstales, K.S., 2008, Documentation for the 2008 Update of the United States National Seismic Hazard Maps: U.S. Geological Survey Open-File Report 2008-1128, 61 p.

Petersen, M.D., Pankow, K.L., Biasi, G., and Meremonte, M.., 2008, What can we learn from the Wells, NV earthquake sequence about seismic hazard in the intermountain west? [abs.]: EOS (Transactions of the American Geophysical Union), v. 89, no. 53, abstract #S51B-1749.

Ponce, D.A., 1997, Gravity data of Nevada: U.S. Geological Survey Digital Data Series DDS-42, 27 p., CD-ROM.

Ponce, D.A., and Glen, J.M.G., 2008, A prominent geophysical feature along the northern Nevada rift and its geologic implications, north-central Nevada: Geosphere, v. 4, no. 1, p. 207–217.

Premo, W.R., Castiñeiras, P., and Wooden, J.L., 2008, SHRIMP-RG U-Pb isotopic systematics of zircon from the Angel Lake orthogneiss, East Humboldt Range, Nevada—is this really Archean crust?: Geosphere, v. 4, no. 6, p. 963–975.

Reed, J.C., Jr., compiler, 1993, plate 1, Map of the Precambrian rocks of the conterminous United States and some adjacent parts of Canada, *in* Reed, J.C., Jr., Bickford, M.E., Houston, R.S., Link, P.K., Rankin, D.W., Sims, P.K., and Van Schmus, W.R., editors., 1993, Precambrian: Conterminous U.S.: Boulder, Colorado, Geological Society of America, The Geology of North America, v. C-2, 657 p., 7 pls.

Rodriguez, B.D., and Williams, J.M., 2008, Tracking the Archean-Proterozoic suture zone in the northeastern Great Basin, Nevada and Utah: Geosphere, v. 4, no. 2, p. 315–328.

Saltus, R.W., and Jachens, R.C., 1995, Gravity and basin depth maps of the Basin and Range Province, Western United States, U.S. Geological Survey Geophysical Investigations Map GP-1012, scale 1:2,500,000.

Simpson, R.W., Jachens, R.C., Blakely, R.J., and Saltus, R.W., 1986, A new isostatic residual gravity map of the conterminous United States with a discussion on the significance of isostatic residual gravity anomalies: Journal of Geophysical Research, v. 91, no. B8, p. 8,348–8,372.

Sims, P.K., Saltus, R.W., and Anderson, E.D., 2005, Preliminary Precambrian basement structure map of the continental United States—an interpretation of geologic and aeromagnetic data: U.S. Geological Survey Open-File Report 2005-1029, 31 p., 1 pl.

Smith, K., Pechmann, J., Meremonte, M., and Pankow, K., *this volume,* Preliminary Analysis of the M_w 6.0 Wells Nevada, Earthquake Sequence.

Stewart, J.H., and Carlson, J.E., 1978, Geologic map of Nevada: Nevada Bureau of Mines and Geology Map, scale 1:500,000.

Thorman, C.H., 1970, Metamorphosed and nonmetamorphosed Paleozoic rocks in the Wood Hills and Pequop Mountains, northeast Nevada: Geological Society of America Bulletin, v. 81, no. 8, p. 2417–2447.

Thorman, C.H. and Brooks, W.E., *this volume,* Bedrock Geology of the Ranges Bounding the Wells Earthquake of February 21, 2008.

Thorman, C.H., Brooks, W.E., Ketner, K.B., and Dubiel, R.F., 2003, Preliminary geologic map of the Oxley Peak area, Elko County, Nevada: Nevada Bureau of Mines and Geology Open-File Report 03-4, scale 1:24,000.

Thorman, C.H., and Ketner, K.B., 1979, West-northwest strike-slip faults and other structures in allochthonous rocks in central and eastern Nevada and western Utah: Rocky Mountain Association of Geologists, Basin and Range Symposium, 1979, Proceedings, p. 123–133.

Thorman, C.H., Ketner, K.B., Brooks, W.E., Snee, L.W., and Zimmerman, R.A., 1991, Late Mesozoic-Cenozoic tectonics in northeastern Nevada, in Raines, G.L., Lisle, R.E., Schafer, R.W., and Wilkinson, W.H., Geology and Ore Deposits of the Great Basin Symposium: Geological Society of Nevada, Reno, 1991, Proceedings, v. 1, p. 25–45.

Tosdal, R.M., Wooden, J.L., and Kistler, R.W., 2000, Geometry of the Neoproterozoic continental breakup, and implications for the location of Nevadan mineral belts, in Cluer, J.K., Price, J.G., Struhsacker, E.M., Hardyman, R.F., and Morris, C.L., editors, Geology and ore deposits 2000—the Great Basin and beyond: Geological Society of Nevada, p. 451-466

Wallace, A.R., Perkins, M.E., and Fleck, R.J., 2008, Late Cenozoic paleogeographic evolution of northeastern Nevada: Evidence from the sedimentary basins: Geosphere, v. 4, no. 1, p. 36–74, doi: 10.1130/GES00114.1.

Zoback, M.L., McKee, E.H., Blakely, R.J., and Thompson, G.A., 1994, The northern Nevada rift—regional tectono-magmatic relations and middle Miocene stress direction: Geological Society of America Bulletin, v. 106, p. 371–382.